Main lessons learnt from 40 years of R&D on iodine source term prediction: Identification of the main parameters governing iodine volatility in PHEBUS FP tests

Loïc Bosland, Karine Chevalier Jabet

Progress in Nuclear Energy 177 (2024) 105473

Contents lists available at ScienceDirect

Progress in Nuclear Energy

journal homepage: www.elsevier.com/locate/pnucene

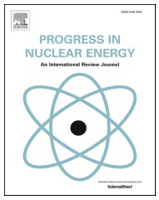

Main lessons learnt from 40 years of R&D on iodine source term prediction: Identification of the main parameters governing iodine volatility in PHEBUS FP tests

Loïc Bosland *, Karine Chevalier-Jabet

Institut de Radioprotection et de Sûreté Nucléaire (IRSN), PSN-RES/SAM/LETR, Cadarache BP 3, 13115, Saint Paul Lez Durance, France

ARTICLE INFO

Keywords:
PHEBUS-FPT tests
Iodine chemistry
Kinetics
Severe accident
ASTEC-SOPHAEROS
Uncertainties

ABSTRACT

Iodine chemistry and phenomenology in the containment has been studied for several decades. The main phenomena leading to the formation of volatile iodine have been identified step by step and their kinetics has been modeled and capitalized over the years in ASTEC-SOPHAEROS IRSN Severe Accident (S.A) code. Recently, the uncertainties for each phenomenon have been quantified and uncertainty propagation calculations have been performed on PHEBUS FPT-0/1/2/3 tests within the objective to identify which phenomena govern iodine volatility. The main highlights from PHEBUS studies are that (1) the sump reactions do not contribute to iodine volatility and (2) the gaseous phase chemical reactions are the main contributor to iodine volatility and (3) only a few gaseous reactions govern iodine volatility in PHEBUS containment. Another objective was to narrow the estimated range of $\%I_{2\_RCS}$ (gaseous iodine fraction coming from the RCS). The results show that, considering 43 uncertain parameters, the iodine volatility plume is compatible with the experimental data whatever $2\% < \%I_{2\_RCS} < 50\%$ that mostly govern iodine volatility in the first days. It also indicates that, as soon as the FP release from the core is stopped and whatever $2\% < \%I_{2\_RCS} < 50\%$, the influence of $\%I_{2\_RCS}$ decreases over time so that the main processes leading to iodine volatility are slowly switched from $\%I_{2\_RCS}$ (short term) to other gaseous phenomena (long term). The influence of $\%I_{2\_RCS}$ on iodine volatility is thus important in the short term but becomes less and less significant in the long term (after several days). A more complete analysis is necessary for reactor applications to identify if the same conclusions can be drawn.

1. Introduction

In the nuclear community, iodine behaviour in the reactor containment has been studied for about 40 years to better predict the Source Term (ST) in case of severe accident (S.A). It has led to multiple studies on iodine behaviour in the sump, in the gaseous phase and on the immersed and dry surfaces (stainless steel, paint and concrete). Performing small-scale experiments has led to set up phenomenological kinetics models able to catch the main trends of each identified phenomenon influencing the containment iodine chemistry in a significant manner. Over the years, all the kinetics models have been implemented and capitalized in the ASTEC-SOPHAEROS S.A code [(Van Dorsselaere and Chatelard al., 2010), (Cantrel and Cousin al., 2014), (Chatelard and Belon al., 2016)]. On top of this modeling approach focused on the development of one model for each phenomenon dealing with iodine chemistry, the intermediate-scale tests PHEBUS-FPT-0/1/2/3 [whose main containment characteristics are shown on Figs. 1–4] were used within the objective to check the reliability and validate the related iodine containment phenomenology (recalled on Fig. 5) with ASTEC-SOPHAEROS [(Girault and Bosland al., 2010), (Girault and Bosland al., 2012), (Weber and Bosland al., 2010), (Haste and Di Giuli, 2015), (Di Giuli and Haste al., 2016)]. Over the years, on top of iodine aerosols, two main families of volatile iodine have been identified to possibly contribute to the Source Term: inorganic iodine (usually considered to be mostly molecular iodine, I_2, even though HOI and HI species could also contribute [(Keller and Duce al., 1970), (Wilhelm, 1982), (Lin, 1980), (Jubin, 1979)]) and organic iodides (CH_3I, C_2H_5I, C_3H_7I, CH_2I_2 …) [(Wren and Ball, 2001), (Taghipour and Evans, 2002), (Parsly, 1971), (Clement and Cantrel al., 2007), (Evans and Palson, 1991)] that are usually summed up as the methyl iodide specie (CH_3I or more generally RI representing organic iodides species) as it was found to be the main one formed under irradiation [(Parsly, 1971), (Clement

* Corresponding author.
E-mail address: loic.bosland@irsn.fr (L. Bosland).

https://doi.org/10.1016/j.pnucene.2024.105473
Received 12 April 2024; Received in revised form 21 August 2024; Accepted 27 September 2024
Available online 3 October 2024

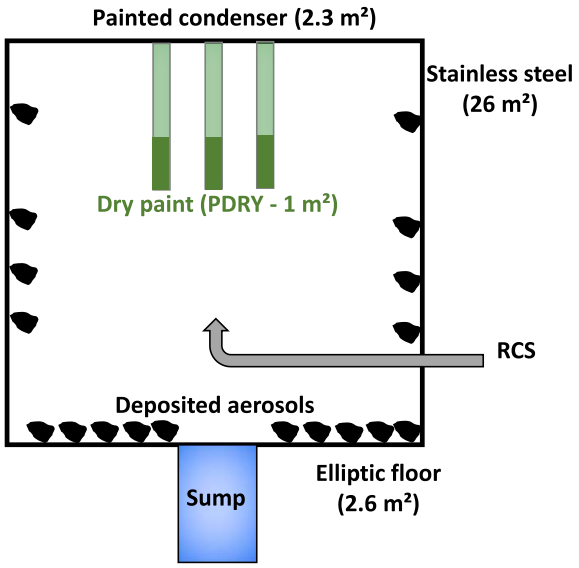

Fig. 1. PHEBUS FPT test containment schematic view.

and Cantrel al., 2007)]. I_2 can come from the reactor coolant system (RCS) but can also be formed by several phenomena in the containment: radiolytic oxidation of iodides ions in the sump and I_2 transfer in the gaseous phase [(Burns and March 1986), (Funke and Zeh al., 1999), (Ashmore and Brown al., 2000), (Guilbert and Bosland al., 2007)], desorption from the paint [(Bosland and Colombani, 2017), (Bosland and Dickinson al., 2014), (Guilbert and Bosland al., 2008)] and stainless steel surfaces [(Funke and Greger al., 1996), (Wren and Glowa al., 1999), (Wren and Glowa, 2001), (Evans and Nugraha, 2002)], radiolytic decomposition of multicomponent iodine soluble (like CsI or CdI_2) and insoluble (AgI) aerosols deposited on dry surfaces [(Bosland and Colombani, 2020a), (Bosland and Leroy al., 2021)], the thermal and radiolytic decomposition of deposited iodine oxides aerosols (IOx) [(Bosland and Leroy al., 2021), (Leroy and Bosland, 2023), (Bosland and Leroy, 2024)]. Volatile organic iodides (RI) can be formed in the containment by sump reactions between dissolved organics and I_2 (Wren and Ball al., 1999), by the iodine-paint interaction in the gaseous phase [(Bosland and Colombani, 2017), (Bosland and Dickinson al., 2014), (Guilbert and Bosland al., 2008)] and are not expected to come from the RCS (Bosland and Colombani, 2020b). They can be also formed by radiolytic reactions between gaseous I_2 and volatile organic compounds (VOCs) [(Bartonicek and Habersbergerova, 1986), (Dickinson and Sims al., 2001)] and from the reaction between adsorbed I_2 on stainless steel surfaces and VOCs [(Postma and Zadovski, 1972), (Adams and Browning al., 1965)] whose modeling still needs some modeling efforts. The results of more than 40 years of research in this area has been capitalized in ASTEC-SOPHAEROS S.A code. Despite a first evaluation of the influence of the model uncertainties on iodine ST calculations in 2014 (Chevalier-Jabet and Cousin al., 2014), new models have been developed since: I_2 and RI-paint interactions (Bosland and Colombani, 2017), IOx thermal and radiolytic decomposition (Bosland and Leroy, 2024) and RI gaseous formation (Bosland and Colombani, 2020b). To better understand the influence of the uncertainties of these new models on iodine ST evaluations, new calculations needed to be performed which is the aim of this paper. In a first approach, the uncertainties for each kinetics model have been estimated. Then, the modeling of iodine chemistry in the containment of the four PHEBUS tests FPT-0/1/2/3 [(Hanniet and Repetto, 1999), (Jacquemain and Bourdon al., 2000), (Gregoire and March al., 2008), (Payot and Haste al., 2010)] has been performed using uncertainty propagation calculations within the objectives to identify which reactions are responsible for the formation of volatile iodine (I_2, RI) and to evaluate the influence of these phenomena over the transient. On top of the kinetics uncertainties, the gaseous iodine fraction coming from the RCS ($\%I_{2\_RCS}$) was added as another uncertain parameter for FPT-0/1/2 because of the possible underestimation of its quantification (Bosland and Leroy, 2024) (for FPT-3, $\%I_{2\_RCS}$ has been well quantified). The calculations have led to identify the main parameters governing iodine volatility in the containment and whose influence and evolution over the transient is described in this

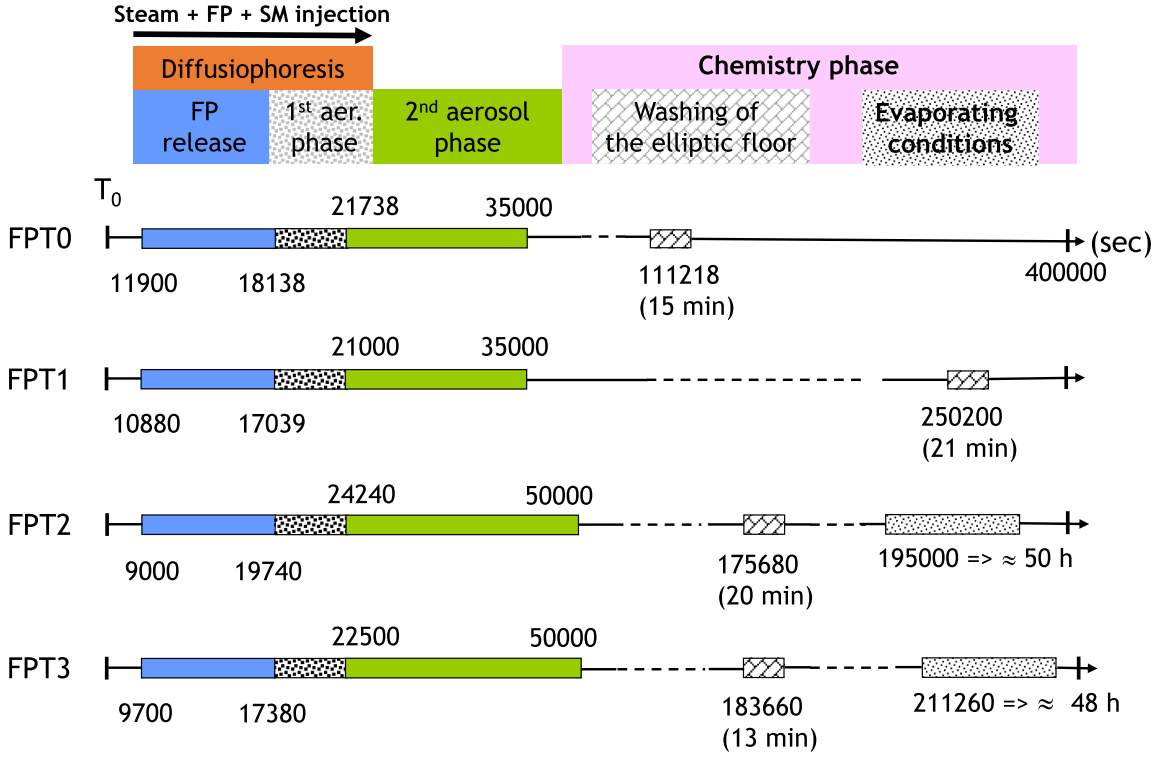

Fig. 2. Simplified PHEBUS FPT tests chronology [32].

paper.

2. Description of the methodology and the calculations

2.1. Brief description of the PHEBUS containment

PHEBUS tests [(Hanniet and Repetto, 1999), (Jacquemain and Bourdon al., 2000), (Gregoire and March al., 2008), (Payot and Haste al., 2010)] containment description is shown on Fig. 1. A simplified chronology of the transient is displayed on Fig. 2 (Bosland and Leroy, 2024) whereas iodine inventory, estimated $\%I_{2\_RCS}$ in PHEBUS FPT tests and washing characteristics are provided in Table 5. The fission products (FP) are injected in the containment from the RCS from ≈10.000 s to ≈ 18.000 s. After this time, the reactor is shut down and the steam injection into the containment is stopped at ≈ 22.000 s. After the containment isolation from the RCS, the aerosol phases lead to the deposition of all types of aerosols on the surfaces, including the elliptic horizontal floor. After one to two days, the washing of this floor is made to transfer the iodine aerosols into the sump and check how it modifies the iodine volatility. The evolution of the containment temperature and relative humidity (RH) is shown on Figs. 3 and 4. While the gaseous temperature was kept almost constant all over the tests for FPT-2/3, it was increased after the floor washing for FPT-0/1. The humidity evolution is also different: while the RH decreases after the washing for FPT-0/1/3, it is increased for FPT-2. The gaseous iodine concentrations was quantified with Maypacks (selective filters that allow to quantify aerosols on the first stage, inorganic iodine on the second stage and organic iodides on the third stage).

2.2. Description of the uncertain parameters and their variation range

Fourty four uncertain parameters were considered in this approach. Their uncertainty range is listed in Table 1 (sump chemistry), Table 2 (chemistry on immersed and dry surfaces) and Table 3 (gaseous phase chemistry). All parameters are independent and direct parameters from SOPHAEROS. If a kinetics parameter is expected to have a potential influence on iodine volatility, it has been selected as an uncertain parameter. A best estimate kinetics (k_{BE}) value was thus defined as well as its variation range according to the literature data on this kinetics and expert's knowledge. As a result, k_{BE} can vary from a factor 2 to 10. % I_{2_RCS} was also considered as an uncertain parameter to cover the uncertainties on its experimental estimation that are mostly due to (1) the missing sampling time on the containment gaseous Maypack (for which the sampling time could represent only ≈ 50% of the degradation time) and (2) to the Maypack operation characteristics that were discussed in a previous paper [32]. Its range varies from 2% to 50% (considering a best-estimate value of 10%).

2.3. Uncertainty propagation method

The Latin Hypercube Sampling method was used for uncertainty propagation, as it offers simplicity and straightforwardness and ensure that every equal/nth interval of probability is sampled once, the randomness of the method lying in the association of sampled values of the uncertain parameters. Given a density probability law for each uncertain parameter, a user chosen size 'n' sampling was performed respecting these laws. Each sample was then fed to ASTEC-SOPHAEROS, yielding in the end as much calculation results (n) as the size of the sample.

Orders statistics, and more precisely the percentiles, were then used to establish the uncertainty range of the outputs. This method has the advantage of not needing the estimation of the density probability function (nature and associated parameters). In this article, the term percentile of a variable refers to the variable value dividing its distribution such that the pth percentile is the value greater than p% of the other values.

For sensitivity analysis, correlation coefficient was used, and more specifically the partial rank coefficient (RPCC), as the ranking allows us to get rid of the assumption of linearity, although the monotonicity hypothesis remains.

The elaboration of the samples and of the calculation results was done using the R platform [(Team, 2022)] and its statistical tools, and more specifically the sensitivity package [(Looss and Da Veiga al., 2023)].

2.4. Description of the distribution laws

Two distribution laws were chosen and compared: the triangle and uniform distributions. In the uniform one, each value of the parameter "k" has the same probability to be chosen whereas in the triangle one,

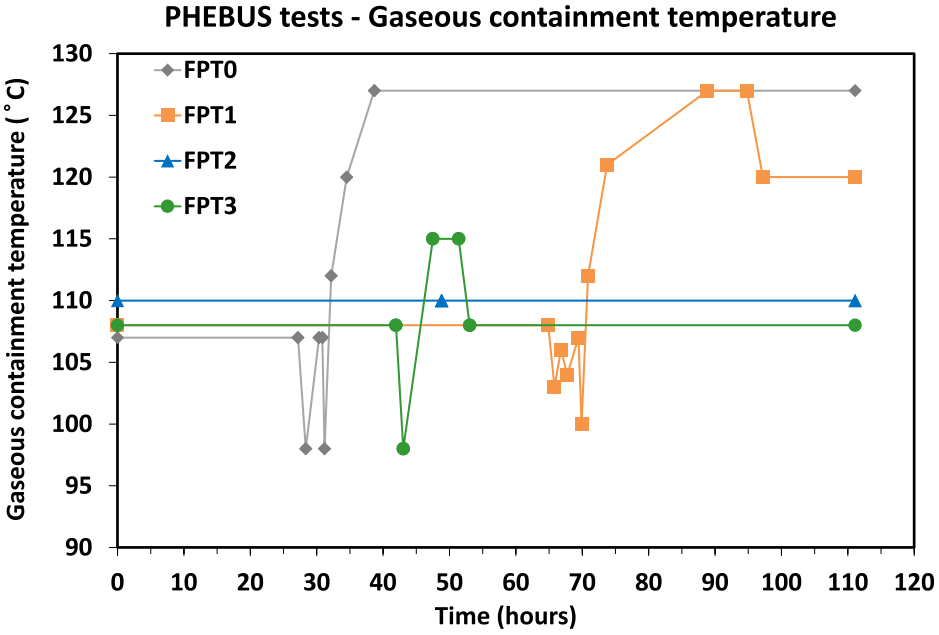

Fig. 3. Gaseous temperature evolution in the PHEBUS FPT tests.

the values close to the best estimate kinetics value (k_{BE}) have a higher probability to be chosen by the sampling (Fig. 6). In case the uncertainty range is large, the triangle distribution function would favor the parameter values that are closer the best-estimate value which could be considered as a more realistic approach. A total of n = 2000 samplings was made for each distribution law.

This number of calculations was chosen because (1) a very good precision (>99%) on the 5%–95% quantiles is ensured (2) a very good precision on the correlation coefficient (RPCC) is also guaranteed and (3) there was no limitations on the calculation time as each calculation takes some seconds only.

In pure random sampling, the Wilks' formula gives a conservative order of magnitude of the needed sample size. For example, if we need a 99% confidence level on the 95% percentile, the sample size "n" should not be lower than 90 (and 460 for 99% percentile). Latin hypercube sampling provides an even better coverage of the variation range, and therefore, combining the use of the LH sampling method and a higher sample size (n = 2000) than the required one is even more precise.

Considering the sensitivity analysis, the critical values (calculated with the Bravais Pearson critical values based on a Student test) above which RPCC coefficients can be considered as relevant is under 0.05 (for a sample size of 2000 and a confidence level of 0.95). Moreover, an estimation of the precision on RPCC (made with the bootstrap method) for gaseous I_2 of FPT-1 at 24h and 96h for the variables having a RPCC >0.4 has been made and was found to be lower than 6%. Therefore, for example, RPCC = 0.50 (±6%) ensures that the related kinetics coefficient has an overall higher influence on iodine volatility than RPCC = 0.4 (±6%) of another kinetics coefficient.

By default, the uniform distribution law was chosen for the calculations and a sensitivity analysis has been performed on the triangle distribution function to check its influence on the results.

2.5. Description of the calculations and analysis of the results

Table 4 describes the performed calculations. As there is no significant experimental uncertainty on $\%I_{2\_RCS}$ for FPT-3, $\%I_{2\_RCS}$ was considered as an uncertain parameter only for FPT-0/1/2. Overall, 26.000 calculations were performed. All the figures and results representing the volatility of iodine highlight the 0.05 (lowest curve), 0.5 (centered curve) and 0.95 (highest curve) percentiles, which indicates that 90% of the results from each set of 2000 calculations are comprised between these two curves (the extreme top >0.95 and bottom <0.05 percentiles are not shown).

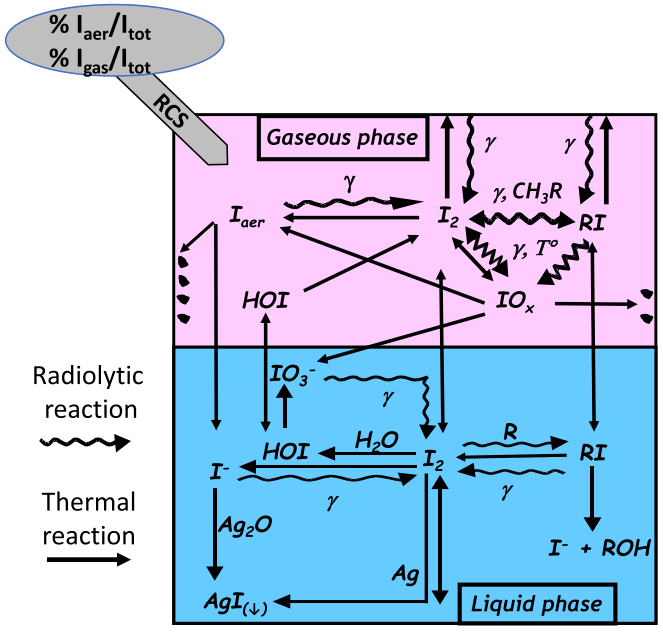

Fig. 5. Phenomenology of iodine behaviour in ASTEC-SOPHAEROS severe accident code.

To highlight which parameters are influent on iodine volatility for a certain time of interest, the choice was made to look at the RPCC. We've mostly looked at the comparison between the modeled and experimental data evolution for the gaseous iodine species evolution (I_2 and RI) and to the influence of the kinetics parameters that (1) are responsible for iodine volatility and (2) that mostly influence this volatility evolution in the short and long-term. RPCC >0 means that an increase of the kinetics parameter of interest leads to an increase of I_2 (or RI) whereas RPCC <0 indicates that an increase of this kinetics parameter leads to a decrease of I_2 (or RI) volatility. In the following sections, we analyze the influence of the kinetics parameters leading to an increase and decrease of I_2/RI.

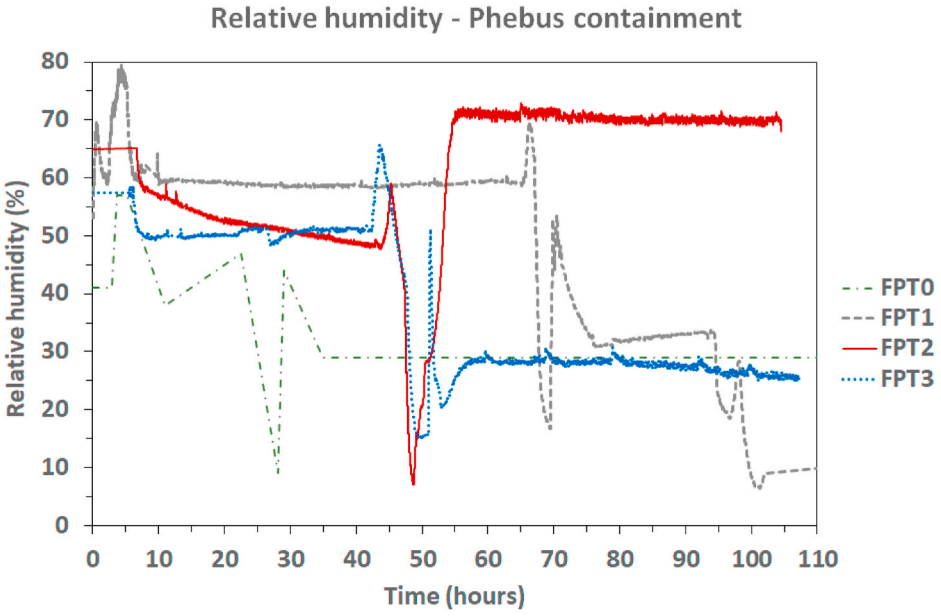

Fig. 4. Relative humidity evolution in the PHEBUS FPT tests.

Table 1
Description of the phenomena, their related kinetic parameter and their variation range (Min/Max) for the sump and mass transfer phenomena.

Parameter	Description of the phenomena	Minimum value considered/Best estimate value	Maximum value considered/Best estimate value
Sump reactions			
k6	I^- thermal oxidation by O_2 (forward reaction)	0.2	5
km6	I^- thermal oxidation by O_2 (reverse reaction)	0.2	5
krhoh	I- oxidation into I_2 by radiolysis (m2 model) + RI radiolytic formation in the sump	0.2	5
Er	I^- oxidation into I_2 by radiolysis (m2 model, backward reaction)	0.71	1.29
k9	RI radiolysis in the sump	0.5	2
k12	RI hydrolysis in the sump	0.5	2
Ag2Oinitial	% of oxidized Ag arriving in the containment	Not considered in this study	
k10	$Ag_2O + I^-$ reaction	0.1	10
k11	$Ag + I_2$ reaction	0.1	10
TMAG2	Coefficient for the AgI maximum layer thickness	0.77	1.28
Mass transfer parameters from the sump and the gaseous phase			
kgI	Individual mass transfer coefficient on the gaseous phase	0.5	2.5
klI	Individual mass transfer coefficient in the sump	1	10

3. Modeling of iodine volatility

In the following sections, it will be mostly looked at the comparison between the experimental data quantified on the Maypacks (volatile inorganic and organic iodine amounts) and their modeling. For inorganic iodine, it is assumed that gaseous I_2 is the main contributor to the experimental data quantified by the Maypacks (even though in some cases a contribution of IO_{xgas} could also contribute as discussed in our previous paper [32] even though it is uncertain and its extent is not known). Organic iodides are modeled by the methyl iodide specie (CH_3I or more generally RI). The choice of looking at gaseous I_2 and RI is guided by the historical understanding of the gaseous iodine phenomenology that was used to set up the selective maypack technology.

Then, the main kinetics parameters contributing to those two output variables all over the transient have been identified and their influence will be shown through the RPCC parameter.

3.1. Influence of the kinetics parameters on inorganic volatility and organic volatility

Figs. 7 and 8 compare the measured inorganic volatility with the "volatile inorganic iodine plume" for FPT-0/1/2/3 whereas Figs. 9 and 10 compare the "RI plume". The overall modeling of the experimental data is well caught by the modeling for all tests. We can observe an underestimation in the long term for the inorganic plume for FPT-0/3 that could come from the IO_{xgas} that are not considered on the maypack in the modeling [32]. Whereas the RI experimental data evolution is well caught for FPT-1/3 all over the transient, it is slightly overestimated for FPT-2 and underestimated in the long term for FPT-0.

It is observed different tendencies over the transient that are well caught by the modeling: for example, for FPT-1/3, whereas inorganic iodine decreases quickly and in a significant manner after the end of the FP release (5.5 h) and until the floor washing, it increases for 2 days for FPT-2 (there are no data for FPT-0 before 20 h but the modeling indicates that it should follow FPT-1/3 tendency).

Another striking observation is the effect of the washing of the floor on iodine volatility: whereas it leads to a significant decrease for FPT-2 (>54.2 h) and no significant effect for FPT-3 (58.7 h), it leads to an increase for FPT-1 (>69.5 h) and FPT-0 (>30.9 h, visible effect only with the modeling as there are not enough experimental data around this time). Similar trends are observed for the effect of the washing on RI volatility. The phenomena governing iodine volatility might thus be different and might evolve depending on the tests and their conditions. The purpose of the next chapter is to identify which gaseous/sump/surfaces kinetics parameters and phenomena govern iodine volatility.

Table 2
Description of the phenomena, their related kinetic parameter and their variation range (Min/Max) for the adsorption and desorption from the immersed and dry surfaces.

Parameter	Description of the phenomena	Minimum value considered/Best estimate value	Maximum value considered/Best estimate value
Adsorption and desorption from immersed and dry surfaces			
kadsI2SWET	I_2 adsorption kinetic on immersed steel	0.2	5
kdesI2SWET	I_2 desorption kinetic from immersed steel	0.2	5
kadsI2PWET	I_2 adsorption kinetic on immersed paint	0.2	4
kdesI2PWET	I_2 desorption kinetic from immersed paint	0.1	10
kadsI2PDRY	I_2 adsorption kinetic on dry paint	0.1	5
kadsRIPDRY	RI adsorption kinetic on dry paint	0.5	2.5
kfastRI	Fast-release kinetics of RI from dry paint	0.5	2
kslowRI	Slow-release kinetics of RI from dry paint	0.2	5
kslowI2	Fast-release kinetics of I_2 from dry paint	0.2	5
kfastI2	Slow-release kinetics of I_2 from dry paint	0.5	2
kx	Coefficient for I_2 adsorption on dry paint	0.5	1.5
ky	Coefficient for I_2 adsorption on dry paint	0.5	1.5
kadsI2SDRY	I_2 adsorption kinetic on dry steel	0.2	5
kdesI2SDRY	I_2 desorption kinetic from dry steel	0.2	5
kI2Fe	Kinetics of I_{2ads} conversion into I_2Fe on the steel	0.2	5
kI2FeOx	Kinetics of I_2Fe conversion into I_2FeOx on the steel	0.2	5
kadsi2aer	I_2 adsorption kinetic on suspended aerosols	0.3	3

3.2. Influence of the sampling law

Even though the results are not shown (as they are not that different), the triangle distribution law leads to a narrower plume than the uniform law whatever the output variable of interest. We might expect a similar result using a normal distribution function instead of the triangle one as both are quite similar. Using the uniform distribution law by default in this work leads to consider a conservative approach for the Source Term evaluation on iodine volatility (broader plume).

Table 3
Description of the phenomena, their related kinetic parameter and their variation range (Min/Max) for the containment gaseous reactions.

Parameter	Description of the phenomena	Minimum value considered/Best estimate value	Maximum value considered/Best estimate value
IOx formation and decomposition in the gaseous phase			
kO3	Air radiolytic products kinetics formation	0.2	5
kO3m	Air radiolytic products	0.2	5
kO3m1	kinetics decomposition	0.2	5
kO3m2		0.2	5
k1	IOx formation	1	5
km1	IO_{xgas} radiolytic decomposition	0.1	10
krdr	$IO_{xaerosol}$ radiolytic decomposition	0.2	5
krdt	Thermal decomposition of	0.2	5
k02	IOx	0.2	5
k03		0.2	5
Formation and decomposition of CH_3I in the gaseous phase			
kCH3Rgas	Radiolytic conversion of I_{2gas} into CH_3I_{gas}	0.2	5
k13	RI radiolytic decomposition into I_2 and IOx	0.25	4
Multicomponent aerosols decomposition			
kImulti	Radiolytic decomposition of suspended and deposited multicomponent aerosols	0.2	5
Gaseous iodine coming from the RCS into the containment			
k_{I2RCS}	% of gaseous iodine coming from the RCS	0.2	5

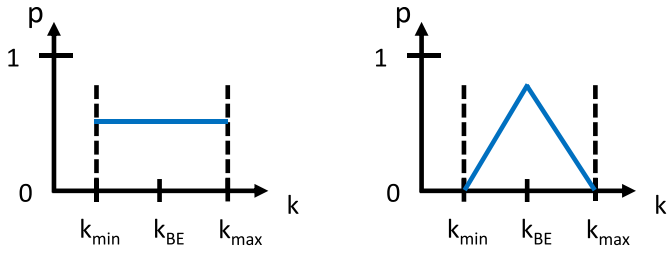

Fig. 6. Comparison of the uniform and triangle distribution functions.

Table 4
Number of calculations performed for each PHEBUS FPT test modeling.

Number of parameters	$\%I_{2\_RCS}$	FPT-0	FPT-1	FPT-2	FPT-3
44	**2% < < 50%**	2000	2000	2000	–
43	**2%**	2000	2000	2000	–
43	**10%**	2000	2000	2000	–
43	**50%**	2000	2000	2000	–
43	**95%**	–	–	–	2000

4. Identification of the main kinetics parameters contributing to iodine volatility

Figs. 11 and 12 show (for FPT-1 as an example) which kinetics parameters are the main parameters governing inorganic and organic iodine volatility at 24.5h (6h before the washing) and 97.7h (end of the test). They are sorted by influence importance. Among the 44 uncertain parameters considered in the calculations, only a few of them are responsible for iodine volatility. This tendency also observed for FPT-0/2/3 all over their transient. Another striking observation is that these main influent parameters all deal with gaseous reactions and heterogeneous surface reactions located in the gaseous phase. The modeling

Table 5
Iodine inventory, estimated $\%I_{2\_RCS}$ in PHEBUS FPT tests and washing characteristics.

	FPT-0	FPT-1	FPT-2	FPT-3
Iodine core inventory (mg)	36	1120	1570	1190
Iodine containment inventory (aerosol + gaseous) (mg)	23	715	885	406
Estimated gaseous iodine mass entering the containment (mg)	>1.4	>34	>1.7	386
Estimated $\%I_{2\_RCS}$/containment inventory (%)	>6.1	>4.8	>1.7	95
Estimated $\%I_{2\_RCS}$/bundle inventory (%)	>3.9	>0.4	>0.1	32.4
Characteristics of the floor washing				
Floor washing time (hours)	30.9	69.5	54.2	58.7
Floor washing duration (min)	15	21	20	13
Washing efficiency (%)	69	92	23	97

also indicates that the uncertainties of the silver/iodine and iodine water reactions (that are retaining iodine effectively in the sump water) do not exhibit a significant effect on iodine volatility in PHEBUS (RPCC close to zero). In fact, the very efficient trapping of iodine in the sump has been highlighted in previous paper [(Simondi-Teisseire and Girault al., 2013)] and is mostly due to: a high Ag/I ratio in FPT-0 and FPT-1 which traps iodine into the sump, an alkaline FPT-2 sump (known to favor I_2 sump decomposition and avoid its transfer to the gaseous phase), and a high amount of gaseous iodine arriving into the FPT-3 containment (95% of the containment inventory) combined with a very low silver mass into the sump (as the control rod was made with B_4C instead of Ag-In-Cd) [40,41,42,43].

From the calculations, the main influent reactions and phenomena on iodine volatility are:

- $\%I_{2\_RCS}$ from the RCS (k_{I2RCS})
- The radiolytic decomposition of I_{aer} (k_{Imulti}) into I_2
- The thermal decomposition of IOx aerosols (k_{02}) into I_2
- The radiolytic conversion of I_2 into CH_3I (k_{CH3R})
- The radiolytic decomposition of RI into I_2 and IOx aerosols (k_{13})
- The adsorption of I_2 on dry paint ($k_{adsI2PDRY}$)
- The transfer of I_2 from the gaseous phase to the sump and surfaces (k_{gI})
- The adsorption of RI on dry paint ($k_{adsRIPDRY}$)
- The release of RI from paint (k_{slowRI})

In the next sections, a more detailed analysis is made about their influence over time on iodine volatility (I_2 and RI).

4.1. Main reactions leading to I_2 formation

Four kinetics parameters were found to be mostly responsible for gaseous I_2 formation. Their influence is explained below.

4.1.1. Influence of $\%I_{2\_RCS}$ over time on I_2 volatility

Fig. 13 shows the influence of $\%I_{2\_RCS}$ in I_2 over time for FPT-1 (left) and FPT-2 (right). This parameter plays a major influence in the very short term for all tests but tends to be less and less influent in the long term. The containment iodine phenomenology (Fig. 5) tends to temper the effect of $\%I_{2\_RCS}$ in the long term, as if the containment memory of $\%I_{2\_RCS}$ would be slowly lost over the days.

4.1.2. Influence of k_{Imulti} over time on I_2 volatility

Fig. 14 shows the influence of k_{Imulti} (decomposition of I_{aer} into I_2) on I_2 over time for FPT-1 (left) and FPT-2 (right). This parameter is gaining in importance as soon as the aerosols are being deposited (<10 h) and until the washing. Then, depending on how efficient the washing is, the effect of this parameter tends to diminish if the washing is efficient (FPT-1) or become a very influent parameter leading to I_2 formation in case of a non-efficient washing (FPT-2) because more aerosols remain on the

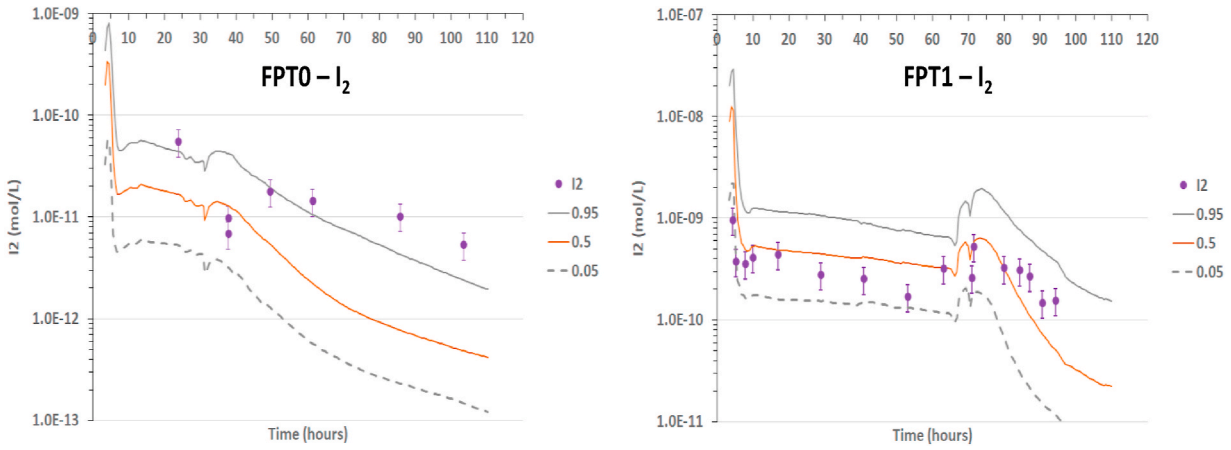

Fig. 7. Comparison data-modeling for I_2 volatility for FPT-0 (left) and FPT-1 (right) considering the 0.05/0.5/0.95 percentiles.

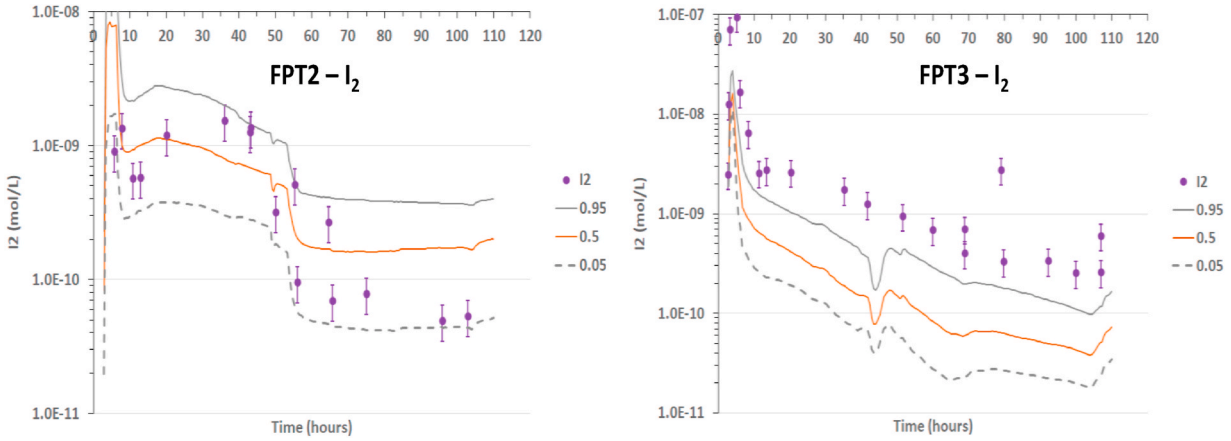

Fig. 8. Comparison data-modeling for I_2 volatility for FPT-2 (left) and FPT-3 (right) considering the 0.05/0.5/0.95 percentiles.

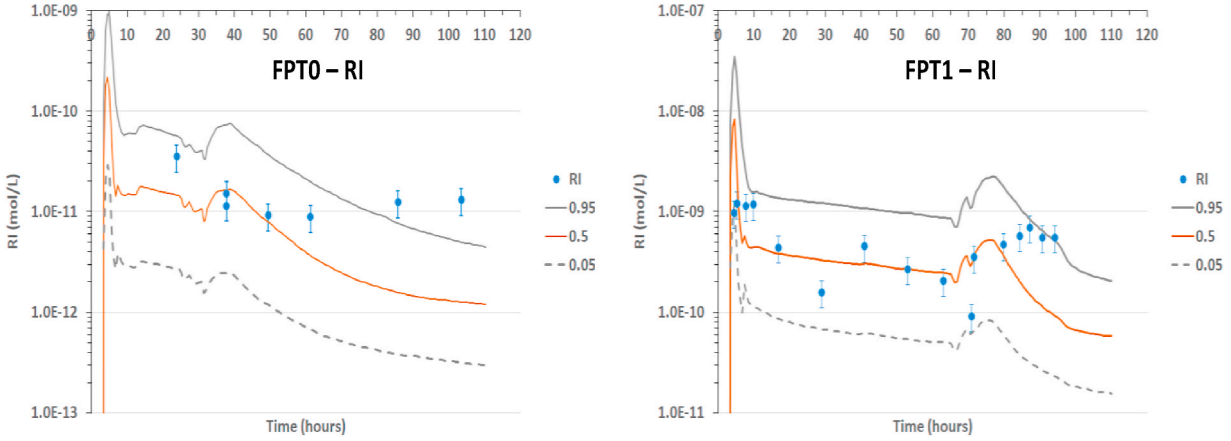

Fig. 9. Comparison data-modeling for RI volatility for FPT-0 (left) and FPT-1 (right) considering the 0.05/0.5/0.95 percentiles.

floor (and are decomposed into gaseous I_2).

4.1.3. *Influence of k_{02} over time on I_2 volatility*

Fig. 15 shows the influence of the thermal decomposition of IOx aerosols into I_2 (k_{02}) on gaseous I_2 over time for FPT-1 (left) and FPT-2 (right). Both RPCCs are positive which means that IOx thermal decomposition is a significant formation source of I_2 until the washing. There is an I_2 peak for FPT-1 at 65h–70h that comes from the decrease of the humidity (Fig. 4) and that leads to a faster IOx decomposition into I_2 (32).

RPCC <0 is considered as a non-relevant tendency in this case as this reaction is a forward reaction only, which means that an increase of its forward kinetics cannot lead to a reduction of one of its product concentrations. RPCC <0 is assumed to come from the indirect correlation of kinetics parameters in the calculations and cannot be considered as relevant.

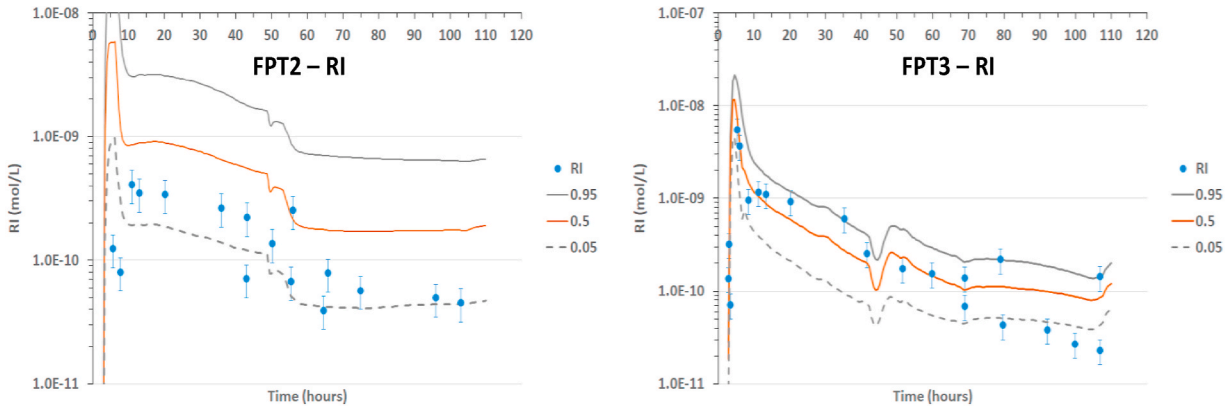

Fig. 10. Comparison data-modeling for RI volatility for FPT-2 (left) and FPT-3 (right) considering the 0.05/0.5/0.95 percentiles.

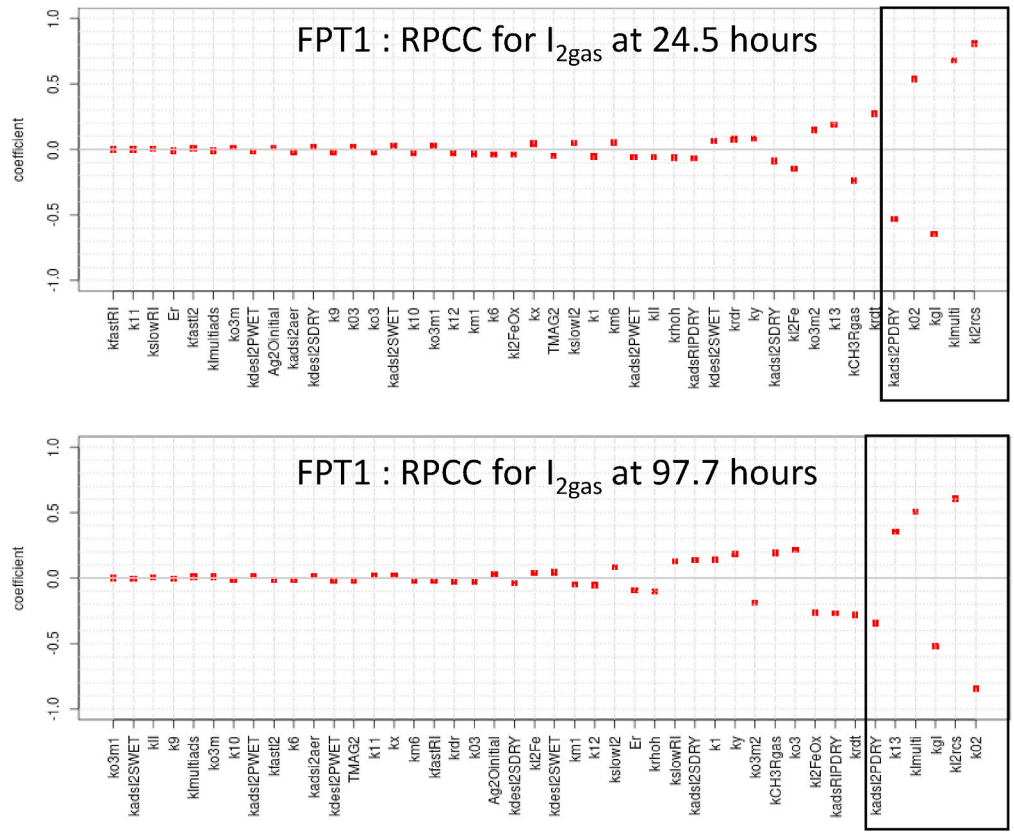

Fig. 11. RPCC for I_{2gas} (FPT-1) at 24.5 h and 97.7 h (end of the test).

4.1.4. *Influence of k_{13} (radiolytic RI decomposition) over time on I_2 volatility*

Even though this reaction leads to the formation of I_2, the influence of this parameter on I_2 formation is significant but in a lesser extent than other parameters (k_{Imulti}, k_{I2_RCS}) but tends to gain in importance after the floor washing for the four PHEBUS tests (no figure shown as $RPCC_{k13} < 0.4$ all over the transient).

4.2. *Main reactions leading to I_2 consumption*

Three reactions kinetics were identified to mostly lead to I_2 consumption.

4.2.1. *Influence of $k_{CH3Rgas}$ over time on I_2 volatility*

Fig. 16 shows that the influence of $k_{CH3Rgas}$ on I_{2gas} is very important at the beginning of the FPT-1/2 tests (at the iodine peak in the containment) and leads to a significant I_{2gas} decrease. Then, its influence is reduced until the washing, which is also observed for FPT-0/3. After the FPT-2 washing, its influence increases again due to the RH increase (Fig. 4) leading to a slower IOx decomposition into I_2 [32]. As I_2 is consumed by the gaseous reaction ($k_{CH3Rgas}$), its relative influence is improved. After the FPT1 washing, RPCC becomes positive which cannot be considered as a relevant result (as this I_{2gas} consumption reaction is a forward reaction that cannot lead to an increase I_{2gas} as explained in section 3.1.3).

4.2.2. *Influence of $k_{adsI2PDRY}$ over time on I_2 volatility*

Fig. 17 shows that the influence of I_2 adsorption kinetics ($k_{adsI2PDRY}$) on gaseous I_2 is significant all over the test for FPT-1 (same result for FPT-2/3) whereas its influence for FPT-0 becomes less significant after

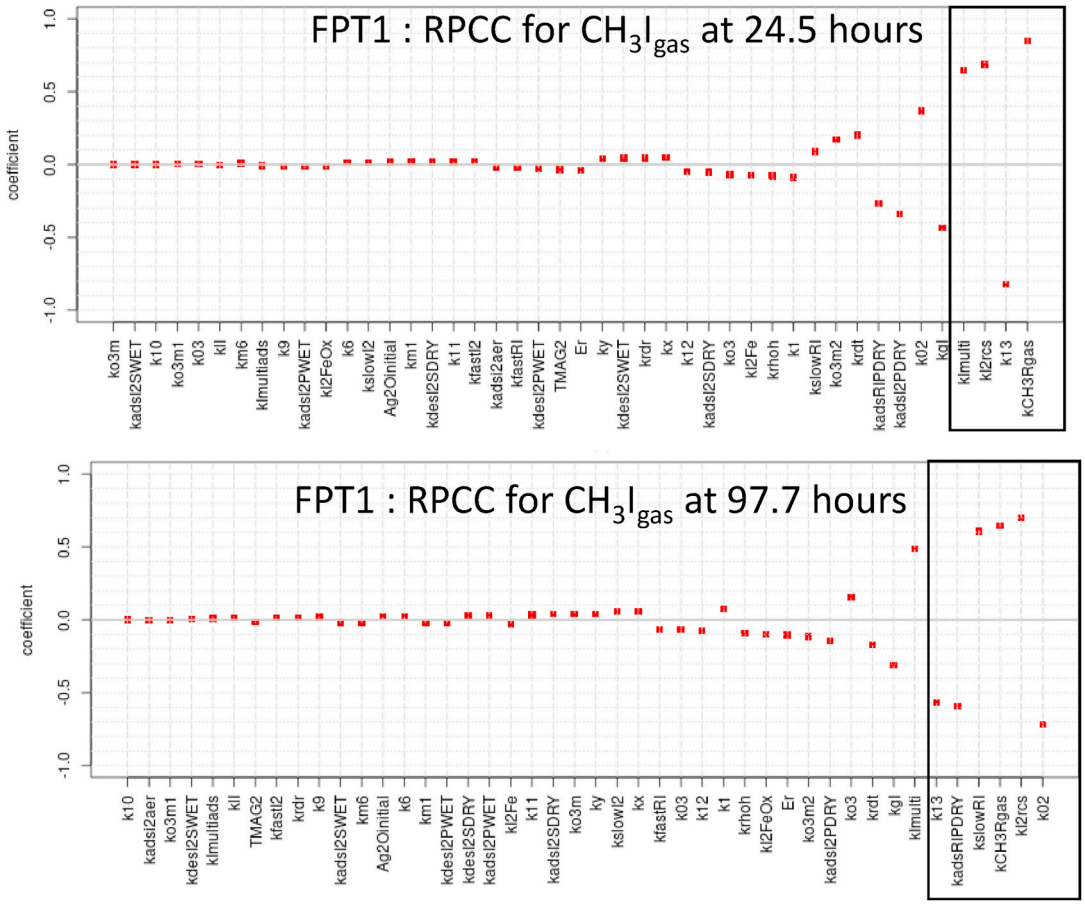

Fig. 12. RPCC for CH_3I_{gas} (FPT-1) at 24.5 h and 97.7 h (end of the test).

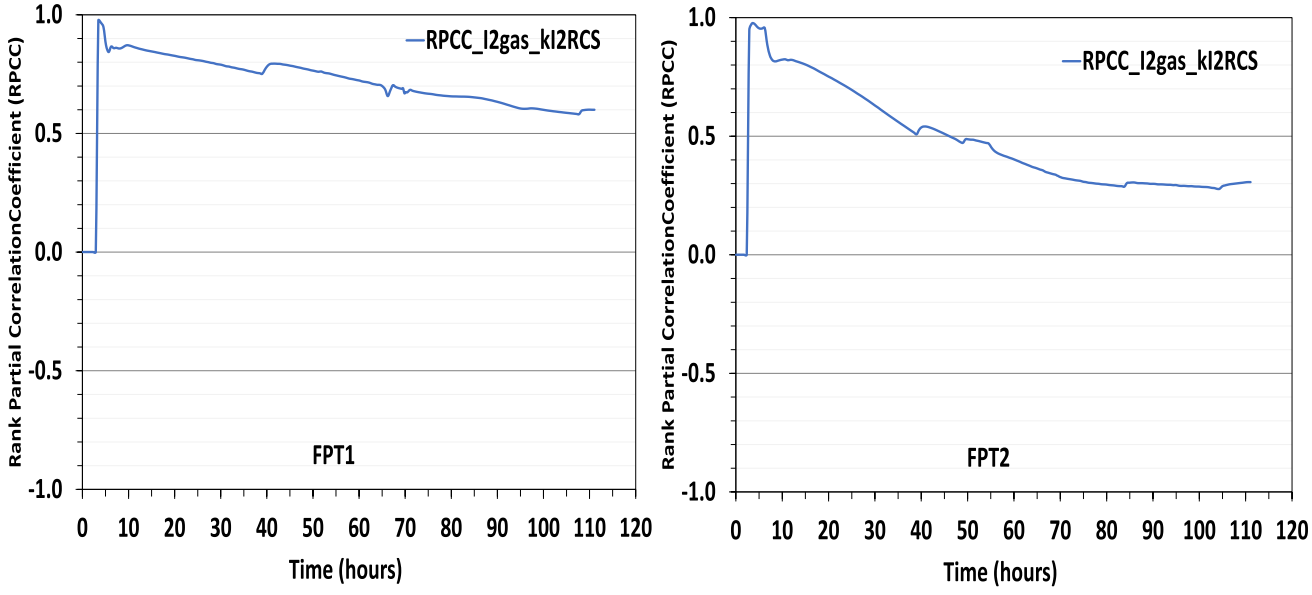

Fig. 13. Evolution of the RPCC of k_{I2RCS} on I_{2gas} for FPT-1 (left) and FPT-2 (right).

the washing (the FPT0 modeled gaseous I_2 concentrations that are observed in the long term are so low that I_2 adsorption on paint becomes insignificant, keeping in mind that the modeling underestimates in a significant manner the data after 80 h). A deeper analysis of the OECD-ESTER data is necessary to evaluate the influence of dry steel surfaces on gaseous RI formation [37,38] and check if this reaction and the related thermalhydraulics conditions could contribute significantly to RI volatility.

4.2.3. *Influence of k_{gI} over time on I_2 volatility*

The transfer of I_2 from the gaseous phase towards the sump and the surfaces (dry paint and dry steel) is also an influent process as RPCC ≈

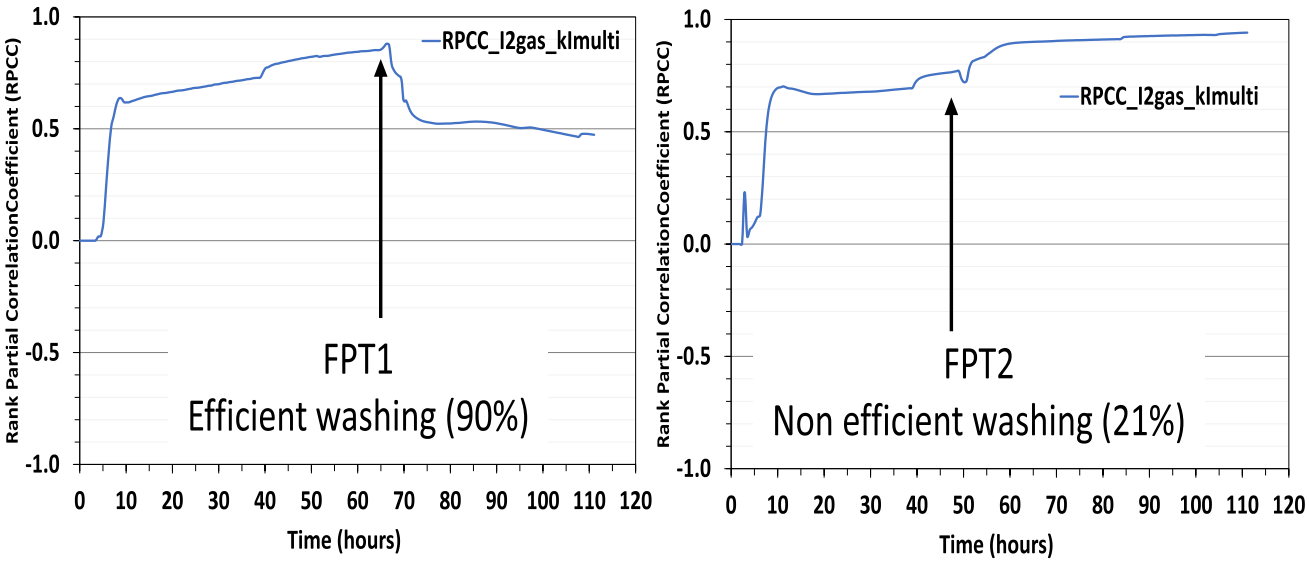

Fig. 14. Evolution of the RPCC of k_{Imulti} on I_{2gas} for FPT-1 (left) and FPT-2 (right).

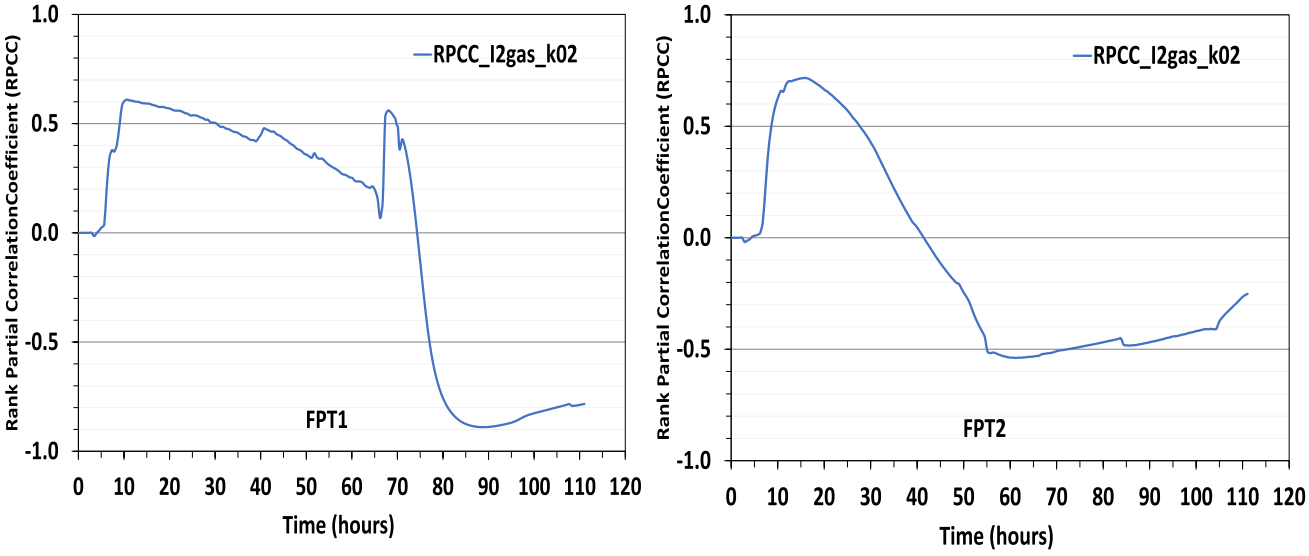

Fig. 15. Evolution of the RPCC of k_{02} on I_{2gas} for FPT-1 (left) and FPT-2 (right).

−0.7 over the whole transient for all tests. As this RPCC does not evolve in a significant during the transient, its evolution was not shown in this paper.

4.3. Main reactions leading to CH_3I formation

Two main routes were identified as leading to CH_3I formation in the gaseous phase.

4.3.1. Influence of $k_{CH3Rgas}$ over time on CH_3I volatility

Fig. 18 shows the influence of $k_{CH3Rgas}$ (conversion of I_2 into RI) on CH_3I over time for FPT-2 (left) and FPT-3 (right). This reaction is one of the main reactions leading to RI formation as $0.5 < RPCC < 1$. A similar observation is made for FPT-0/1.

4.3.2. Influence of k_{slowRI} over time on CH_3I volatility

The second important reaction dealing with RI formation is the slow RI formation from the paint that gains in importance for all PHEBUS tests in the long run (example for FPT-3 on Fig. 19 (right)). This is consistent with the decreasing concentration of I_2 all over FPT-3 (Fig. 8, which leads to a lower RI formation by $k_{CH3Rgas}$ on Fig. 19 (left)) whereas the iodine mass adsorbed onto the paint increases in such manner that the RI formation from the paint slowly gains in importance. This k_{slowRI} effect is less pronounced for FPT-2 as the washing is not efficient so that the proportion of CH_3I formed by the gaseous reaction ($k_{CH3Rgas}$) remains important in the long run.

4.4. Main reactions leading to CH_3I consumption

Three main kinetics were found to decrease significantly CH_3I volatility.

4.4.1. Influence of k_{13} (radiolytic RI decomposition) over time on CH_3I volatility

Fig. 20 shows the influence of k_{13} (radiolytic RI decomposition into) on CH_3I over time for FPT-1 (left) and FPT-2 (right). This reaction has a major effect on gaseous RI consumption (same tendency for FPT-0/3).

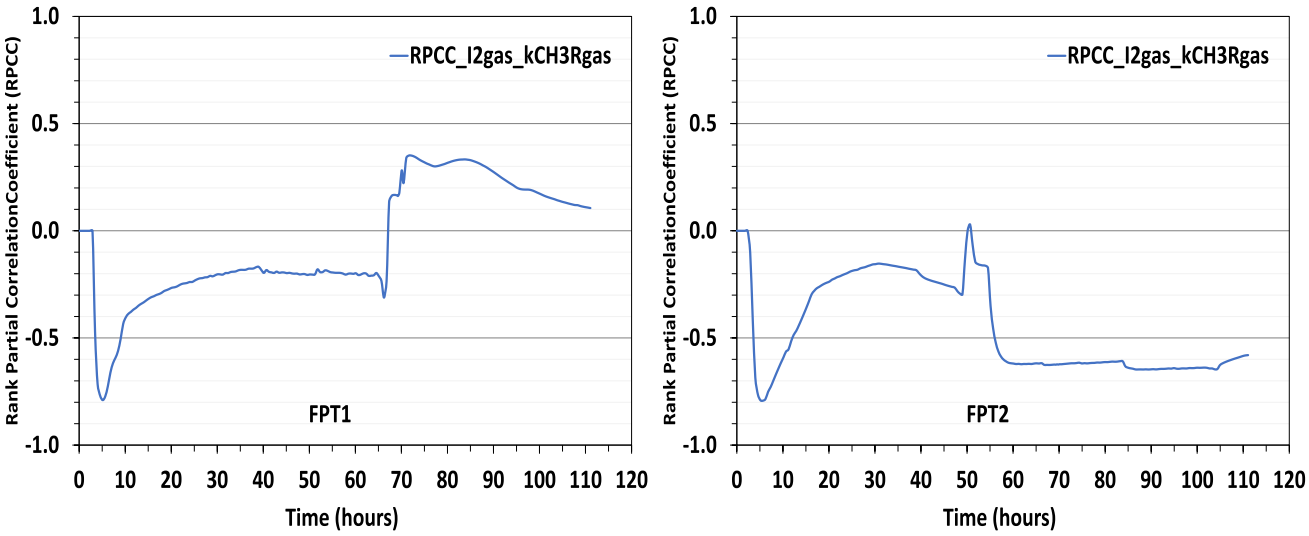

Fig. 16. Evolution of the RPCC of $k_{CH3Rgas}$ on I_{2gas} for FPT-1 (left) and FPT-2 (right).

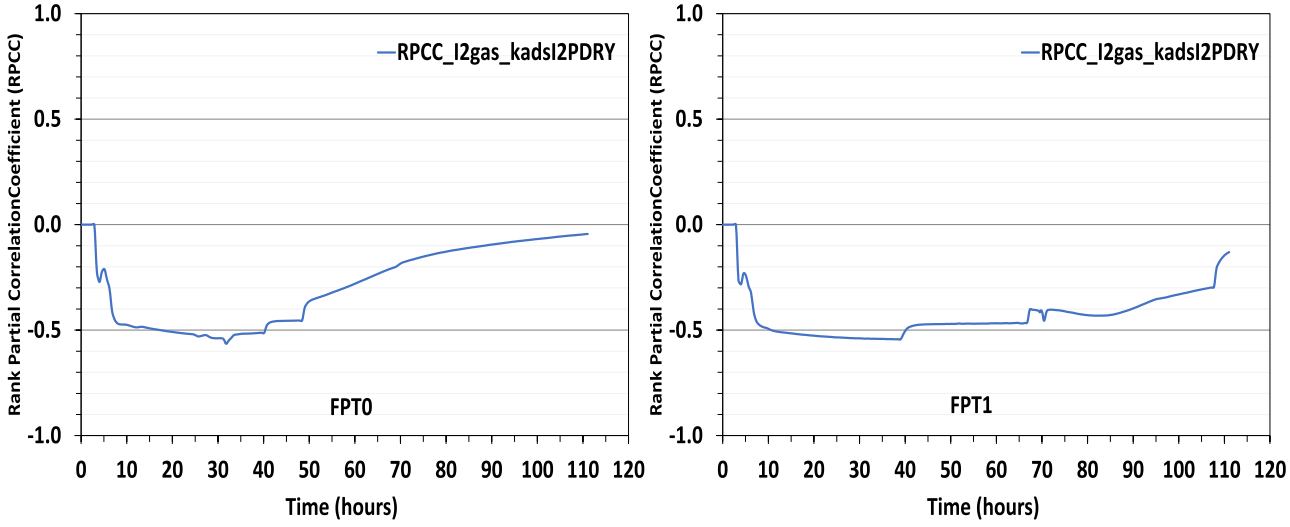

Fig. 17. Evolution of the RPCC of $k_{adsI2PDRY}$ on I_{2gas} for FPT-0 (left) and FPT-1 (right).

4.4.2. *Influence of $k_{adsRIPDRY}$ (adsorption of RI on paint) over time on CH_3I volatility*

Fig. 21 shows that RI adsorption on paint ($k_{adsRIPDRY}$) is a reaction of secondary importance compared to RI decomposition reaction, but its influence tends to become more and more important over the transients, especially after the washing.

4.4.3. *Influence of k_{gI} over time on CH_3I volatility*

The transfer of CH_3I from the gaseous phase towards the sump and the dry paint surface is also an influent process as RPCC ≈ -0.5 over the whole transient for all tests. As this RPCC does not evolve in a significant during the transient, its evolution was not shown in this paper.

These results indicate which phenomena are the main ones leading to the formation/consumption of organic and inorganic iodine volatile species. It has been shown in a previous paper [32] that $\%I_{2\_RCS}$ could have been higher than initially quantified (from 1% to 30%). This approach has shown that $\%I_{2\_RCS}$ is one of the main significant parameters leading to gaseous I_2, particularly in the short and mid-term. Nevertheless, these results do not allow to refine or estimate a narrower range for $\%I_{2\_RCS}$. Complementary calculations have thus been performed to try to estimate a narrower range of $\%I_{2\_RCS}$. Instead of defining $\%I_{2\_RCS}$ as an uncertain parameter (like the 43 others uncertain parameters of Table 1, Tables 2 and 3), three new sets of uncertainty propagation calculations were performed, making a sensitivity study on $\%I_{2\_RCS}$ for FPT-0/1/2 (Table 4, the value for FPT-3 is well known and does not deserve such approach). In these three sets of calculations, $\%I_{2\_RCS}$ is not an uncertain parameter but a fixed value (2%, 10% or 50%). The results are shown below.

5. Sensibility analysis on $\%I_{2\_RCS}$

These calculations were performed to identify any incompatible values for $\%I_{2\_RCS}$, so that the estimation of a compatible range could be narrowed. Figs. 22–24 show the plume for I_2 for FPT-0/1/2 considering the lowest (2%) and highest (50%) value for $\%I_{2\_RCS}$ (the 10% case would lie in between and is not shown to simplify and reduce the figures number).

In the very short term, $\%I_{2\_RCS}$ has a strong influence on I_2 (and CH_3I) for FPT-0/1/2: a multiplication of $\%I_{2\_RCS}$ by 25 (from 2% to 50%) leads to an increase of I_2 by more than an order of magnitude.

In the long term, the influence of $\%I_{2\_RCS}$ on I_2 volatility is reduced (as already observed in Fig. 13) in such manner that a large range of %

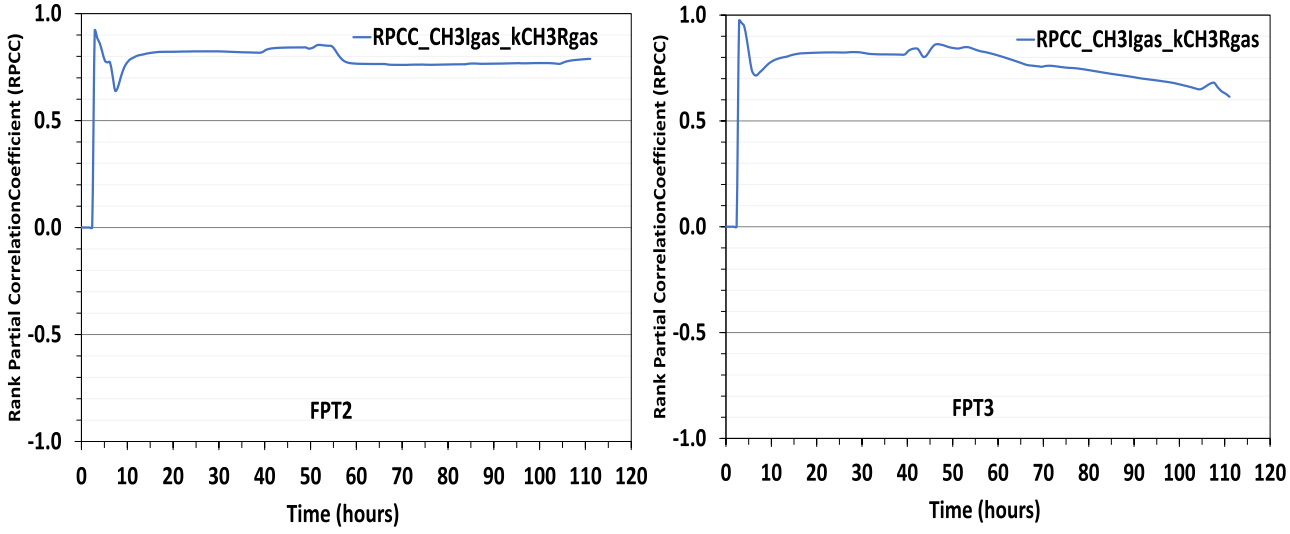

Fig. 18. Evolution of the RPCC of $k_{CH3Rgas}$ on CH_3I_{gas} for FPT-2 (left) and FPT-3 (right).

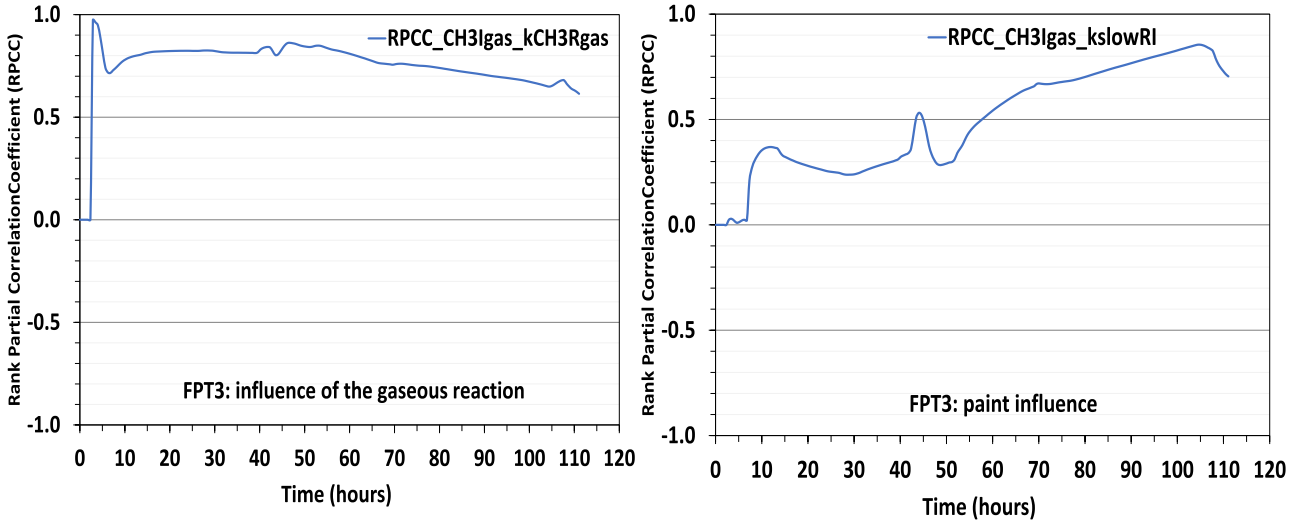

Fig. 19. Evolution of the RPCC of $k_{CH3Rgas}$ (left) and k_{slowRI} (right) on CH_3I_{gas} for FPT-3.

I_{2_RCS} remains compatible with the inorganic iodine experimental data. Even though $\%I_{2\_RCS} = 50\%$ seems to be an upper compatible value with the experimental data, this approach indicates that whatever the initial $\%I_{2\_RCS}$, the iodine volatility in the PHEBUS containment slowly converge toward a steady state whose level depends on the thermal-hydraulics conditions (temperature, RH, dose rate). It is like if $\%I_{2\_RCS}$ would not be influent anymore after some days. A similar conclusion can be drawn for RI volatility, even though the gaseous radiolytic reaction kinetics ($I_2 => CH_3I$) has still to be confirmed by ESTER tests. A complementary work is also necessary to evaluate the influence of a refined RI formation reaction (including the effect of stainless steel) on these results.

6. Conclusions and perspectives

Iodine volatility in the containment of the PHEBUS FPT tests have been modeled with ASTEC-SOPHAEROS. The uncertainties of each kinetics model have been quantified and uncertainty propagation calculations were performed to highlight which phenomena are responsible for inorganic and organic iodine formation and decomposition processes. Because of the high Ag/I ratio and/or the alkaline sump and/or a high $\%I_{2\_RCS}$, the PHEBUS sump has acted as an iodine sink, a tendency that is caught by the modeling. Among the 44 uncertain parameters, only a few of them govern iodine volatility. They all deal with gaseous chemical reactions: IOx aerosols thermal decomposition into I_2, multi-component iodine aerosols (I_{aer}) radiolytic decomposition into I_2, I_2 and CH_3I radiolytic decomposition into IOx aerosols, I_2 radiolytic conversion into CH_3I, I_2/CH_3I adsorption processes on surfaces and their transfer to the sump/surfaces and the slow RI radiolytic release from the paint.

One of the objectives of this work was to narrow the range of compatible values of $\%I_{2\_RCS}$ with the PHEBUS data. Because of all the other uncertainties, this objective could not be completed. Nevertheless, considering $\%I_{2\_RCS}$ as an uncertain parameter has led to highlight that it is a major parameter leading to high level of gaseous iodine in the short term whereas, after some days, its influence was reduced in a significant manner. The phenomenology acts as if the containment would slowly forget the initial value of $\%I_{2\_RCS}$, because of all the other chemical processes that take place in the containment. After several days, the experimental data tend to show that a quasi-steady-state is reached whose level depends mostly on the thermal-hydraulics conditions (temperature, RH, gaseous dose rate) whatever the initial value of $\%I_{2\_RCS}$ whose influence on iodine volatility is progressively significantly

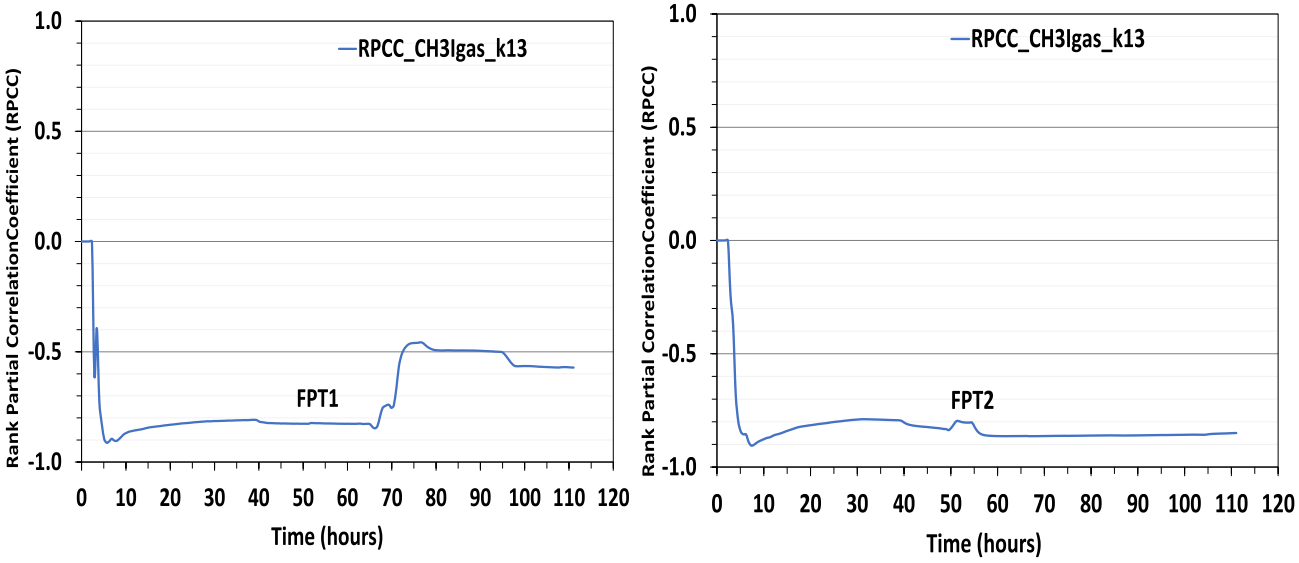

Fig. 20. Evolution of the RPCC of k_{13} on CH_3I_{gas} for FPT-1 (left) and FPT-2 (right).

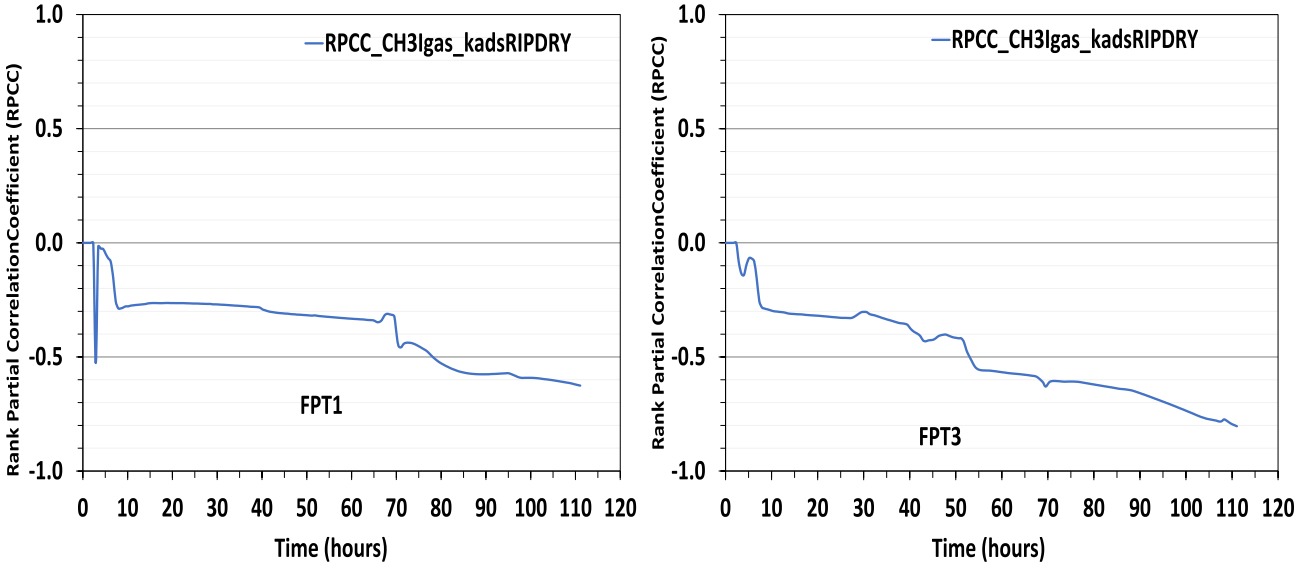

Fig. 21. Evolution of the RPCC of $k_{adsRIPDRY}$ on CH_3I_{gas} for FPT-1 (left) and FPT-3 (right).

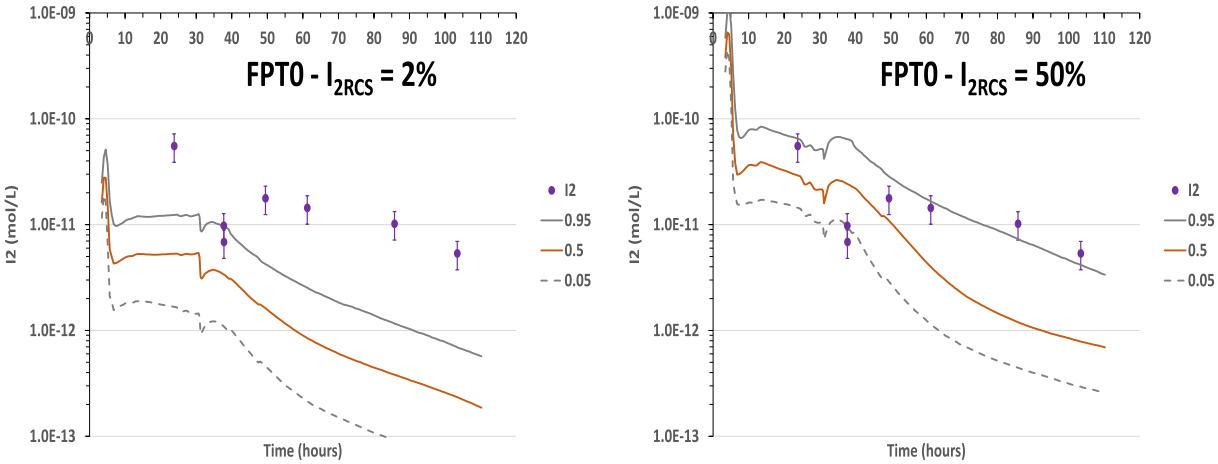

Fig. 22. Comparison data-modeling for I_2 volatility for FPT-0 considering a low $\%I_{2RCS}$ (2%, left) and a high $\%I_{2RCS}$ (50%, right) with the 0.05/0.5/0.95 percentiles.

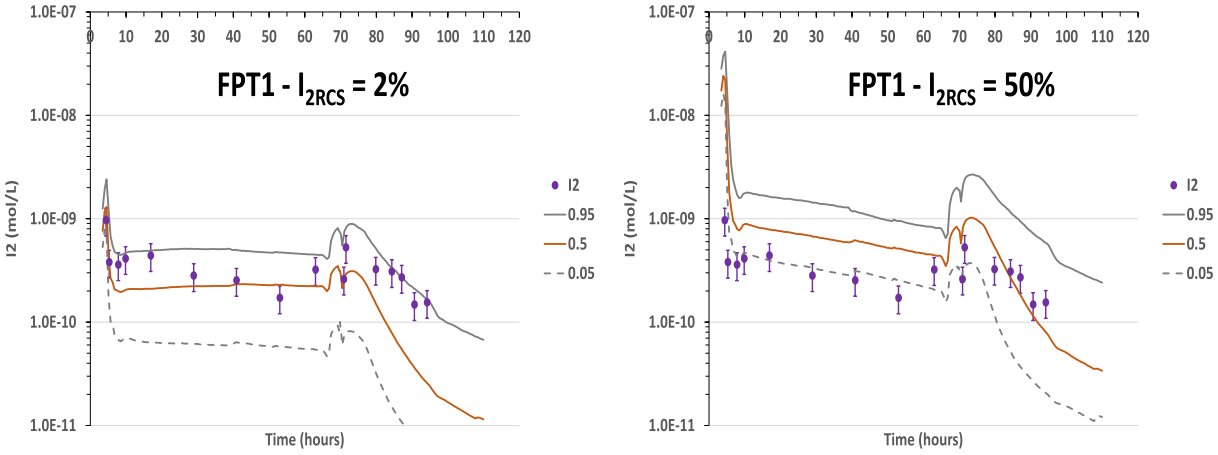

Fig. 23. Comparison data-modeling for I_2 volatility for FPT-1 considering a low $\%I_{2RCS}$ (2%, left) and a high $\%I_{2RCS}$ (50%, right) with the 0.05/0.5/0.95 percentiles.

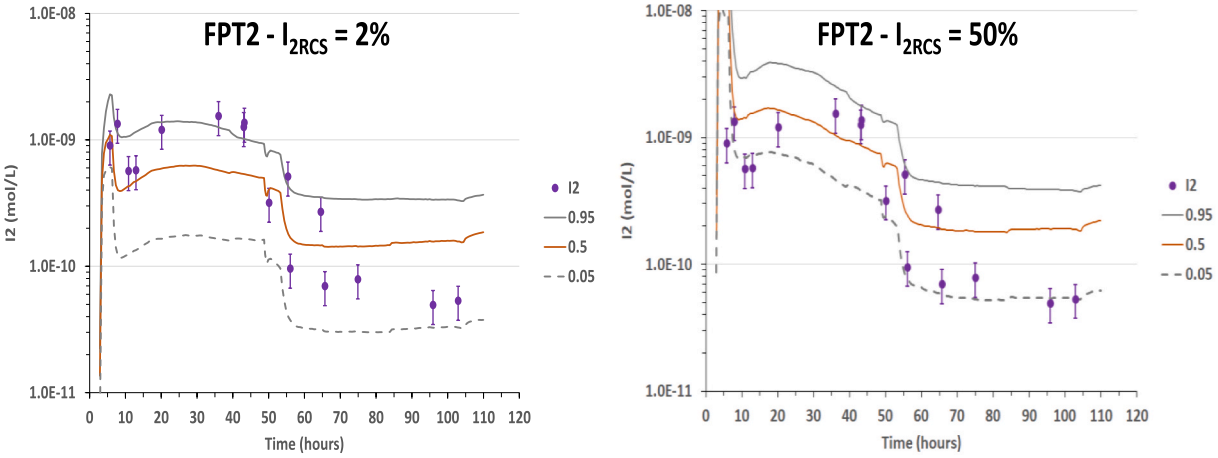

Fig. 24. Comparison data-modeling for I_2 volatility for FPT-2 considering a low $\%I_{2RCS}$ (2%, left) and a high $\%I_{2RCS}$ (50%, right) with the 0.05/0.5/0.95 percentiles.

reduced over time.

A deeper analysis of the OECD-ESTER data is necessary to evaluate the influence of dry steel surfaces on gaseous RI formation [37,38] and check if this reaction could contribute significantly to RI volatility. Another gaseous contribution to the inorganic Maypack stage (I_2) and potentially the final organic Maypack stage (RI) is the amount of IOx_{gas} that are formed in the containment before they nucleate into aerosol. An analysis and discussion about the influence of this phenomena is available in another recent paper to be published [32]. A complementary work is also necessary to evaluate if the same tendencies and conclusions could be drawn for reactor applications, depending on the scenarios and the evolution of the thermal-hydraulics parameters.

CRediT authorship contribution statement

Loïc Bosland: Writing – review & editing, Writing – original draft, Visualization, Validation, Supervision, Software, Resources, Project administration, Methodology, Investigation, Formal analysis, Data curation, Conceptualization. **Karine Chevalier-Jabet:** Writing – review & editing, Validation, Software, Methodology, Conceptualization.

Declaration of competing interest

The authors declare that they have no known competing financial interests or personal relationships that could have appeared to influence the work reported in this paper.

Data availability

The authors do not have permission to share data.

Acknowledgments

Authors acknowledge Nathalie GIRAULT for her contribution to the PHEBUS FPT-0/1/2/3 project through its continuous support to the tests executing and interpretation over the years and to Laurent CANTREL for his contribution to the definition of the min-max range of the uncertain parameters.

References

Adams, R.E., Browning, W.E., et al., 1965. The release and adsorption of methyl iodide in the HFIR maximum credible accident. ORNL-TM-1291.

Ashmore, C.B., Brown, D.J., et al., 2000. Measurements of the radiolytic oxidation of aqueous CsI using a sparging apparatus. Nucl. Tech. 129 (3), 387–397. https://doi.org/10.13182/NT00-A3069.

Bartonicek, B., Habersbergerova, A., 1986. Investigation of the formation possibilities of alkyl iodides in nuclear power plants. Radiat. Phys. Chem. 28 (5/6), 591–600.

Bosland, L., Colombani, J., 2017. Study of iodine releases from Epoxy and Polyurethane paints under irradiation and development of a new model of iodine-Epoxy paint interactions for PHEBUS and PWR severe accident applications. J. Radioanal. Nucl. Chem. 314 (2), 1121–1140. https://doi.org/10.1007/s10967-017-5458-9.

Bosland, L., Colombani, J., 2020a. Study of the radiolytic decomposition of CsI and CdI_2 aerosols deposited on stainless steel, quartz and Epoxy painted surfaces. Ann. Nucl. Energy 141, 107241. https://doi.org/10.1016/j.anucene.2019.107241.

Bosland, L., Colombani, J., 2020b. Review of the potential sources of organic iodides in a NPP containment during a severe accident and remaining uncertainties. Ann. Nucl. Energy 140, 107127. https://doi.org/10.1016/j.anucene.2019.107127.
Bosland, L., Dickinson, S., et al., 2014. Iodine-paint interactions during nuclear reactor severe accidents. Ann. Nucl. Energy 74, 184–199. https://doi.org/10.1016/j.anucene.2014.07.016.
Bosland, L., Leroy, O., 2024. Modeling of the decomposition of Iodine oxides aerosols (IOx) in the containment and consequences on the understanding of volatile iodine behaviour in the containment. Submitted to Progress in Nuclear Energy.
Bosland, L., Leroy, O., et al., 2021. Study of the stability of CsI and iodine oxides (IOx) aerosols and trapping efficiency of small aerosols on sand bed and metallic filters under irradiation. Prog. Nucl. Energy 142, 104013. https://doi.org/10.1016/j.pnucene.2021.104013.
Burns, W.G., March, W.R., 1986. The thermal and radiolytic oxidation of aqueous I⁻ and the hydrolysis and disproportionation of aqueous I_2. AERE-R-10767.
Cantrel, L., Cousin, F., et al., 2014. ASTEC V2 severe accident integral code: fission product modelling and validation. Nucl. Eng. Des. 272, 195–206. https://doi.org/10.1016/j.nucengdes.2014.01.011.
Chatelard, P., Belon, S., et al., 2016. Main modelling features of ASTEC V2.1 major version. Ann. Nucl. Energy 93, 83–93. https://doi.org/10.1016/j.anucene.2015.12.026.
Chevalier-Jabet, K., Cousin, F., et al., 2014. Source term assessment with ASTEC and associated uncertainty analysis using SUNSET tool. Nucl. Eng. Des. 272, 207–218. https://doi.org/10.1016/j.nucengdes.2013.06.042.
Clement, B., Cantrel, L., et al., 2007. State of the art report on iodine chemistry. OECD-NEA-CSNI-R 2007, 1.
Di Giuli, M., Haste, T., et al., 2016. SARNET benchmark on Phébus FPT3 integral experiment on core degradation and fission product behaviour. Ann. Nucl. Energy 93, 65–82. https://doi.org/10.1016/j.anucene.2016.01.046.
Dickinson, S., Sims, H.E., et al., 2001. Organic iodine chemistry. Nucl. Eng. Des. 209, 193–200. https://doi.org/10.1016/S0029-5493(01)00402-2.
Evans, G., Nugraha, T., 2002. A study of the kinetics of I_2 deposition on stainless steel sampling lines. Nucl. Tech. 140 (3), 315–327. https://doi.org/10.13182/NT02-A3342.
Evans, G., Palson, A.S., 1991. ACE bench-scale studies of iodine volatility and interaction with EPOXY painted surfaces. In: Proceeding of the Third CSNI Workshop on Iodine Chemistry in Reactor Safety. Tokaï Mura, September, 11th-13rd, JAERI 92-012/NEA/CSNI/R(91)15.
Funke, F., Greger, G.U., et al., 1996. Iodine - steel reactions under severe accident conditions in light-water reactors. Nucl. Eng. Des. 166, 357–365. https://doi.org/10.1016/S0029-5493(96)01253-8.
Funke, F., Zeh, P., et al., 1999. Radiolytic oxidation of molecular iodine in the containment atmosphere. OECD Workshop on Iodine Aspects of Severe Accident Management 79–89. Vantaa, Finland, May 18-20.
Girault, N., Bosland, L., et al., 2010. LWR severe accident simulation fission product behavior in FPT-2 experiment. Nucl. Tech. 169 (3), 218–238. https://doi.org/10.13182/NT10-A9375.
Girault, N., Bosland, L., et al., 2012. LWR severe accident simulation: iodine behaviour in FPT2 experiment and advances on containment iodine chemistry. Nucl. Eng. Des. 243, 371–392. https://doi.org/10.1016/j.nucengdes.2011.11.011.
Gregoire, A.C., March, P., et al., 2008. FPT-2 final report. IRSN/DPAM/DIR 2008 - 272 - Report PHEBUS-FP IP/08/579.
Guilbert, S., Bosland, L., et al., 2007. Radiolytic oxidation of iodine in the containment at high temperature and dose rate. In: International Conference on Nuclear Energy for New Europe (NENE). September, 10 - 13, Portorose, Slovenia.
Guilbert, S., Bosland, L., et al., 2008. Formation of organic iodide in the containment in case of a severe accident. Transactions of the American Nuclear Society, Annual Meeting, June, 08 - 12 Anaheim 98, 291–292. United States.
Hanniet, N., Repetto, G., 1999. FPT-0 final report. CEA/IPSN/DRS/SEA/PEPF - Report PHEBUS PHPF IP/99/423.
Haste, T., Di Giuli, M., et al., 2015. Iodine benchmarks in the SARNET network of excellence. J. Nucl. Eng. Radiat. Sci. 2, 021022. https://doi.org/10.1115/1.4031652.
Jacquemain, D., Bourdon, S., et al., 2000. FPT-1 final report. CEA/IPSN/DRS/SEA/PEPF - rapport SEA 1/100 - Report PHEBUS FP IP/00/479.
Jubin, R.T., 1979. A literature survey of methods to remove Iodine from off-gas streams using solid sorbents. ORNL/TM-6607.
Keller, J.H., Duce, F.A., et al., 1970. Hypoiodous acid: an airborne inorganic iodine species in air-steam mixtures. In: 11th AEC Air Cleaning Conference. Richland, Washington - 31st August - 03rd September.
Leroy, O., Bosland, L., 2023. Study of the stability of iodine oxides (IxOy) aerosols in severe accident conditions. Ann. Nucl. Energy 181, 109526. https://doi.org/10.1016/j.anucene.2022.109526.
Lin, C.C., 1980. Chemical behavior of radioiodine in BWR systems. J. Inorg. Nucl. Chem. 42 (8), 1093–1099. https://doi.org/10.1016/0022-1902(80)80416-7.
Looss, B., Da Veiga, S., et al., 2023. Sensitivity: global sensitivity analysis of model outputs. R package version 1.29.0. https://CRAN.R-project.org/package=sensitivity.
Parsly, L.F., 1971. Chemical and Physical Properties of Methyl Iodide and its Occurrence under Reactor Accident Conditions. ORNL-NSIC-82.
Payot, F., Haste, T., et al., 2010. FPT-3 final report. DPAM/DIR-2010-148 - PF IP/10/587.
Postma, A.K., Zadovski, R.W., 1972. Review of organic iodide. Formation under accident conditions in water-cooled reactors. United States Atomic Energy, Commission Report WASH-1233.
Simondi-Teisseire, B., Girault, N., et al., 2013. Iodine behaviour in the containment in Phébus FP tests. Ann. Nucl. Energy 61, 157–169. https://doi.org/10.1016/j.anucene.2013.02.039.
Taghipour, F., Evans, G.J., 2002. Modeling of Iodine radiation chemistry in the presence of organic compounds. Rad. Chem. and Chem. 64, 203–213. https://doi.org/10.1016/S0969-806X(01)00495-9.
Team, R.C., 2022. R: A Language and Environment for Statistical Computing. R Foundation for Statistical Computing, Vienna, Austria. https://www.R-project.org.
Van Dorsselaere, J.P., Chatelard, P., et al., 2010. Validation status of the ASTEC integral code for severe accident simulation. Nucl. Tech. 170 (3), 397–415. https://doi.org/10.13182/NT10-A10326.
Weber, G., Bosland, L., et al., 2010. ASTEC, COCOSYS, and LIRIC interpretation of the iodine behavior in the large-scale Thai test iod-9. J. Eng. Gas Turbines Power 132 (11). https://doi.org/10.1115/1.4001295.
Wilhelm, J.G., 1982. Iodine filters in nuclear installations. Commission of European Communitites - Contract 1178-80-12 L/V.
Wren, J.C., Ball, J.M., 2001. LIRIC 3.2 an updated model for iodine behaviour in the presence of organic impurities. Radiat. Phys. Chem. 60, 577–596. https://doi.org/10.1016/S0969-806X(00)00385-6.
Wren, J.C., Ball, J.M., et al., 1999. The interaction of iodine with organic material in containment. Nucl. Tech. 125 (3), 337–362. https://doi.org/10.13182/NT99-A2952.
Wren, J.C., Glowa, G.A., 2001. Kinetics of gaseous iodine uptake onto stainless steel during iodine-assisted corrosion. Nucl. Tech. 133 (1), 33–49. https://doi.org/10.13182/NT01-A3157.
Wren, J.C., Glowa, G.A., et al., 1999. Corrosion of stainless steel by gaseous I_2. J. Nucl. Mater. 265, 161–177. https://doi.org/10.1016/S0022-3115(98)00504-2.